Quaternary Science Reviews 207 (2019) 49–63

Contents lists available at ScienceDirect

Quaternary Science Reviews

journal homepage: www.elsevier.com/locate/quascirev

Inferring critical transitions in paleoecological time series with irregular sampling and variable time-averaging

M. Allison Stegner [a, *], Zak Ratajczak [a], Stephen R. Carpenter [a, b], John W. Williams [c]

[a] Department of Integrative Biology, University of Wisconsin-Madison, Madison, WI 53706, USA
[b] Center for Limnology, University of Wisconsin-Madison, Madison, WI 53706, USA
[c] Department of Geography, University of Wisconsin-Madison, Madison, WI 53706, USA

ARTICLE INFO

Article history:
Received 8 July 2018
Received in revised form
13 December 2018
Accepted 13 January 2019

Keywords:
Quaternary
Paleolimnology
Global
Data treatment
Data analysis
Vegetation dynamics
Abrupt change
Critical transitions
Regime shifts
Resilience indicators

ABSTRACT

Many ecosystems have abruptly changed in the past and may again in the future, yet prediction and inference of mechanisms causing abrupt changes remains challenging. Critical transitions are one such mechanism, occurring when systems with alternative states cross a threshold. Such transitions are associated with a loss of resilience, often signaled by increasing variability or autocorrelation over time. However, critical transitions are difficult to distinguish from other causal mechanisms, and detection of resilience loss in sedimentary archives can be confounded by time-averaging and discontinuous sampling. Here, we simulate woodland-grassland regime shifts resulting from critical transitions and other mechanisms. We then test the diagnostic ability of two widely-used resilience indicators, standard deviation and autocorrelation time, after alterations common in sedimentary records: time averaging, discontinuous sampling, and varying sedimentation rates. Standard deviation—but not autocorrelation time—still distinguishes gradually forced critical transitions from other regime shifts when sedimentation rates are constant, and can be robust to abrupt changes in sedimentation rate. Unfortunately, shifts in standard deviation alone are rarely definitive evidence of critical transitions. Under exponential sedimentation regimes, which are common in younger upper-column sediments, neither resilience indicator is effective. Discontinuous sampling weakened the strength of resilience indicators. A demonstrative analysis of abrupt early Holocene deforestation recorded at Steel Lake, Minnesota showed signals consistent with resilience loss during early Holocene aridification. Hence, signals of resilience loss can be recovered from sedimentary archives, but efficacy varies among indicators and sedimentation regime. High-resolution and multi-proxy records remain essential to inferring causes, while process-based time series modeling such as this can be calibrated to systems of interest to explicitly test hypotheses about abrupt change causes.

© 2019 Elsevier Ltd. All rights reserved.

1. Introduction

In the last century, we have witnessed major, and in many cases unexpected, ecological changes as a consequence of high-magnitude and accelerating anthropogenic impacts on the globe (Barnosky et al., 2012; Steffen et al., 2015a). Given future projections for climate change, land conversion, human resource use, and other ecological stressors, we have reason to expect more ecosystem regime shifts—rapid and persistent changes in state—leading to fundamental changes in ecosystem function and services (Barnosky et al., 2012; Hughes et al., 2013; Steffen et al., 2015b). Emerging questions about these trends could potentially be addressed using long ecological time series to search for signals of resilience loss prior to regime shifts (Scheffer et al., 2015), but such efforts are complicated by data features common in temporal ecology, including data gaps, time-averaging, and other confounding processes (Bestelmeyer et al., 2011; Wolkovich et al., 2014; Ratajczak et al., 2018). In this paper, we use simulated time series to assess approaches for detecting changes in resilience and infer critical transitions versus other mechanisms of regime shift.

Predicting when and where regime shifts will take place is complicated by the fact that relationships between ecological state variables (e.g., tree cover, species richness, dominant taxa) and external driver variables (e.g., temperature, anthropogenic nutrient

* Corresponding author. Department of Biology, Stanford University, 371 Serra Mall, Stanford, CA 94305, USA.
E-mail address: mstegner@wisc.edu (M.A. Stegner).

https://doi.org/10.1016/j.quascirev.2019.01.009
0277-3791/© 2019 Elsevier Ltd. All rights reserved.

inputs) can take many forms (Bestelmeyer et al., 2011; Williams et al., 2011; Ratajczak et al., 2018). In the simplest case, driver and state variables are linearly related, so a change in driver leads to a proportional ecological state change. In systems with nonlinear driver-state relationships, when the system is near a threshold, a small change in driver leads to a disproportionately large change in state. In some cases, simply reverting to previous driver levels fails to reverse the change in state (Fig. 1) (Scheffer et al., 2001, 2015). This kind of hysteretic change implies that the ecosystem could exist in one of multiple quasi-stable states (Scheffer et al., 2001, 2015). As the environment changes, the current ecosystem state becomes unstable, and the system passes through a critical transition into a new quasi-stable state. In the paleoecological literature, where long ecological time series are common, ecological regime shifts caused by an interaction of external drivers with internal processes are referred to as intrinsic regime shifts, and can include both critical transitions and reversible thresholds (Williams et al., 2011). Conversely, ecological regime shifts caused by abruptly changing external drivers, such as climate, are usually referred to as extrinsic regime shifts (Williams et al., 2011; Seddon et al., 2014, 2015). Identifying critical transitions and hysteretic systems is important, because the resulting regime shifts are much more difficult to reverse and indicate that small changes in drivers can lead to large changes in ecosystem state.

The statistical signature of resilience loss prior to critical transitions in time series is well known from theory (Carpenter and Brock, 2006; Scheffer et al., 2009, 2015). As an ecosystem approaches a threshold (or bifurcation point), it recovers more slowly from small perturbations, a phenomenon known as critical slowing down (Scheffer et al., 2015). Critical slowing down is marked by increased variance and autocorrelation of time series measured for ecosystem processes or components. These statistical changes in time series are collectively known as 'resilience indicators,' because critical transitions occur when resilience of an ecosystem state is lost (Scheffer et al., 2015). The theory of resilience indicators for ecosystems is robust and growing but experimental tests are few. Some examples include laboratory experiments (Dai et al., 2012; Veraart et al., 2012), whole-ecosystem experiments (Carpenter et al., 2011; Pace et al., 2017; Ratajczak et al., 2017; Wilkinson et al., 2018), detailed time and space observations of ecological collapses (Rindi et al., 2017), and analyses of well-understood transitions in long paleoclimatic time series (Lenton, 2011). Thus, time series statistics (local estimates of variance, autocorrelation, or eigenvalues) indicate changes in resilience and may provide warnings of impending critical transition.

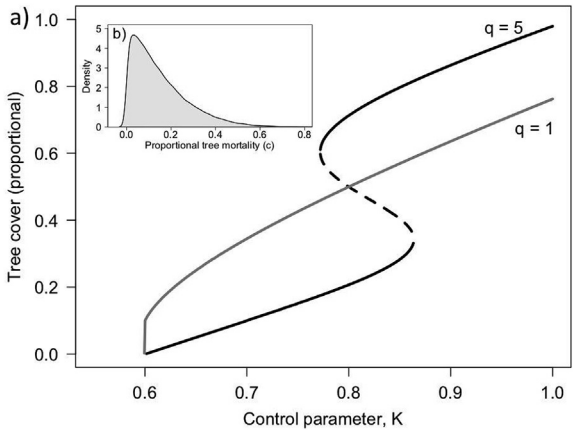

Fig. 1. Fold Bifurcation for Woodland-Grassland Model. a) Fold bifurcation of the models used to generate simulated time series. Solid lines denote stable states, whereas dashed lines are an unstable state. Black colored lines correspond to a system with alternative states and hysteresis. Note that for this system, as *K* (a surrogate for precipitation) decreases, a high tree-cover state eventually reaches a threshold where high tree cover is no longer a stable state of the system. If *K* drops below this threshold, the system will begin a critical transition to a grassland state. The grey line shows the system without alternative states, which was used to generate simulations for the non-critical scenario. Note that for all values of *K*, the system without alternative states has only one possible stable equilibrium. b) Beta distribution used to generate proportional tree mortality, *c*.

Long ecological time series have the potential to reveal changes in resilience at broad scales of space and time by documenting past regime shifts, through analyses of driver-state relationships (Ratajczak et al., 2018) to understand underlying processes, and statistical analyses intended to indicate resilience loss prior to past critical transitions (Thomas, 2016). Paleoecological and paleoenvironmental time series retrieved from continuous depositional environments (e.g. lakes, mires, and estuarine and marine sediments) are well-suited to evaluating signals of resilience and regime shift precursors because of their long duration (10^2–10^7 years), often continuous sedimentation, fine temporal resolution—typically decades, though in some cases years (Goring et al., 2012)—and the availability of multiple biological and geochemical proxies, enabling study of multiple dimensions of past environmental and ecological change. Regime shifts are common features of such records (e.g., Williams et al., 2011; Minckley et al., 2012; Seddon et al., 2014; Spanbauer et al., 2014; Seddon et al., 2015; Bunting et al., 2016; Spanbauer et al., 2016; Belle et al., 2017; Beck et al., 2018). Furthermore, thousands of sediment core records are available for analysis and are widely accessible in public databases like the Neotoma Paleoecology Database (www.neotomadb.org), the European Pollen Database (www.europeanpollendatabase.net), the NOAA National Centers for Environmental Information (www.ncdc.noaa.gov/data-access/paleoclimatology-data) and PANGAEA (www.pangaea.de). When ecosystems have undergone regime shifts in the past—perhaps even multiple times—it may be possible to identify causes of regime shifts and driver-state thresholds, which can be used to anticipate similar transitions in the future (Allen and Breshears, 1998; Randsalu-Wendrup et al., 2016; Thomas, 2016; Belle et al., 2017).

However, attempts to detect critical transitions in long ecological time series face three common challenges: time-averaging, discontinuous sampling, and irregular intervals between samples. Although these challenges are particularly relevant for paleoecological proxies sampled from sedimentary archives, they are general to analyses of long ecological time series. Lake sediments are time-averaged by mixing processes during particulate transport and deposition (Webb, 1993); the amount of time-averaging depends mostly on rate of sediment accumulation and varies among depositional environments, with deposition times for small temperate lakes ranging from ~0.2 to ~300 years per centimeter, with a mean of ~13 yrs/cm (Goring et al., 2012). Uppermost lake sediments are less compacted than deeper horizons, and more compacted layers represent more time per unit depth—thus, time-averaging increases with depth. Paleoecologists typically sample cores discontinuously, at regular depth intervals, because sampling often begins before age-depth relationships are established by radiometric dating and age-depth models (Blaauw and Christen, 2011; Bronk Ramsey, 2009). If depth is non-linearly related to time, samples can be irregularly spaced through time. Paleoecological sampling designs often invest extra effort in achieving high-resolution sampling of regime shifts or other targeted events, resulting in uneven sampling (e.g. Booth et al., 2012). Time-averaging and irregular sampling are both expected to alter the statistical signatures of ecological change and hinder diagnostic analyses of the processes that drove that change. While interpolation is a common answer to irregular sampling, interpolation

fundamentally changes the autocorrelation and variance of a time series (Rehfeld et al., 2011; Carstensen et al., 2013; Mudelsee, 2014; Thomas, 2016) and may thereby interfere with estimates of resilience indicators.

In this study, we conducted a series of data simulations designed to assess how signals of gradually and abruptly forced critical transitions in long ecological time series are transformed by sedimentary processes and typical paleoecological sampling designs, and what diagnostic information is retained after transformation. We: (1) built a simple woodland-grassland model capable of hysteretic and non-hysteretic transitions driven by changes in precipitation and fire; (2) simulated time series of gradually forced critical transitions, abruptly forced critical transitions, gradually forced non-critical transitions, and no change; (3) altered the data by imposing common sedimentation models (linear sedimentation, exponential, and broken-stick linear), and common paleoecological sampling schemes (regular intervals by depth, and targeted sampling of regime shifts); and (4) applied standard resilience indicators that are often used to predict and diagnose gradually forced critical transitions. We also included a real-world example, using reconstructed woody cover data (Williams et al., 2009) of a woodland-grassland regime shift at Steel Lake, Minnesota, to illustrate how this approach can be used to test for resilience loss prior to critical transitions in observational records of regime shifts. Although the analyses focus on vegetation events recorded in lake sediments by fossil pollen records as a case study, the approach and results are relevant to many kinds of paleoecological and paleoclimatic proxies and, indeed, to many kinds of long ecological time series.

2. Methods

2.1. Woodland-grassland model

To simulate gradually forced critical transitions, abruptly forced critical transitions, gradually forced non-critical transitions, and time series with no change in mean state, we developed a simple woodland-grassland model (Fig. 1a) that includes several realistic processes governing tree-cover and which has similar features to models of critical transitions in forest-savanna-grassland systems (e.g. Anderies et al., 2002; Staver and Levin, 2012; Staal et al., 2015; Ratajczak et al., 2017). The model time step is annual. The model is spatially implicit but the intended spatial scale is a landscape on the order of a 10^1–10^2 km radius, which matches typical estimates of pollen source area. The model only describes tree cover (T) but assumes that areas not occupied by trees are occupied by grasses. We used a discrete time model, given by the equations:

$$T_{t+1} = T_t + f(T_t, K_{t+1}) + \lambda_{t+1} \quad (1)$$

Tree cover changes due to deterministic tree expansion and contraction, given by the function $f()$ and environmental noise, denoted by λ (equation (1)).

Deterministic tree cover $f(T,K)$ dynamics follow:

$$f(T, K) = r\,T\,(K - T) - c_t\,T\,(h^q / [h^q + T^q]) \quad (2)$$

Tree cover expansion depends on current tree cover at time step t (T_t) and carrying capacity, K (equation (2)). The first set of terms describes tree growth, which follows a linear logistic model, where maximum intrinsic growth rate (r) is fixed. K is treated as the external driver variable or control parameter, with the assumption that K changes slowly over time and is unaffected by tree cover. Conceptually, K is meant to capture climate, with higher values of K indicating greater water availability. This assumption is consistent with observations that precipitation controls maximum tree cover in many terrestrial regions with a mean annual precipitation less than approximately 1200 mm yr^{-1} (Sankaran et al., 2005; Williams et al., 2009; Eldridge et al., 2011; Staal et al., 2015).

The second set of terms in equation (2) represent mortality due to fire. We assume that a single ignition occurs per year. Fire intensity is represented by c_t and is stochastic to account for background variation in fuel moisture, temperature, and wind-speed. We used a beta distribution to generate values of c_t, because this distribution is flexible and bounded by 0 and 1 (Fig. 1b). The spatial extent of each fire depends on tree cover. Compared to grasses, trees generate less of the finer fuels that are the primary fuel source in many grassland-woodland ecosystems. Greater tree cover usually results in lower grass production, and therefore, further fuel reductions (Eldridge et al., 2011; Ratajczak et al., 2017). Fire spread depends on presence of adjacent patches with fuels adequate to carry fire (Abades et al., 2014). Therefore, when tree cover is low, the connectivity between flammable patches is higher, allowing fire to travel across most of the landscape. However, if tree cover exceeds a threshold, grass-dominated patches become isolated, making it unlikely that fire will spread over much of the landscape (Abades et al., 2014). This "percolation threshold" has been documented in many systems, and usually occurs somewhere between 40 and 60% tree cover (e.g. Abades et al., 2014; van Nes et al., 2018). We represent this fire percolation threshold using a non-linear function, where spatial extent of fire decreases non-linearly if tree-cover exceeds h. This approach follows other simple models of transitions between fire-prone grassy ecosystems and woodlands with lower burned area (Staver and Levin, 2012; Staal et al., 2015). The steepness of changes in tree mortality below h increases with the values of the steepness parameter, q.

Red noise, which captures stochastic environmental fluctuations unrelated to fire, follows the equation of Steele (1985):

$$\lambda_{t+1} = \sigma\,[\,\phi\,\lambda_t + (1\text{-}\phi^2)^{1/2}\,\varepsilon\,] \quad (3)$$

where σ is the standard deviation of red noise, ϕ is the lag-1 autocorrelation coefficient, and ε is white noise with mean = 0 and standard deviation = 1. We set $\phi = 0.05$, based on the lag-1 autocorrelation of annual precipitation in instrumental records (Carpenter et al., 2017), and set $\sigma = 0.005$.

We used plausible parameter values based on contemporary observations of grasslands and woodlands at the prairie-woodland ecotone in the Great Plains of North America (Appendix A). K ranges from 0 to 1, where a value of 1 indicates that the entire ecosystem can become tree-covered. For the r parameter, we used 0.25, based on published rates of large-scale woody plant expansion when fire has been suppressed (Barger et al., 2011; Ratajczak et al., 2017). The stochastic calculation of c_t uses a beta distribution with a mean of 0.15, variance of 0.015, and resulting shape parameters of $\alpha = 1.125$ and $\beta = 6.375$ (Fig. 1b). In keeping with observations (Ratajczak et al., 2017), this parameterization allows fires to remove most woody vegetation over several years, when grasses cover more than half of the landscape. To match the observation of a fire percolation threshold around proportion tree cover = 0.5, we set h to a value of 0.5 so that tree mortality due to fire increases when proportional tree cover falls below 0.5. This parametrization falls in the middle range of similarly structured models (Staver and Levin, 2012; Staal et al., 2015; van Nes et al., 2018). We determined the steepness parameter, q, through experimentation, with the goal of simulating a range of ecological behavior. For smaller values of q (1–3), the relationship between tree cover and tree loss from fires is a linear to slightly sigmoidal relationship. At larger values of q (~4–8) the relationship becomes a sigmoid and at very large values (>8), starts to approximate a step change or block function. For our

default parameterization, we gave q an intermediate value of 5, which is high enough to generate the alternative states that have been inferred from empirical data (Ratajczak et al., 2017). For our parameterization of regime shifts that are non-critical transitions, we used a value of one, which results in a model that produces non-hysteretic responses to varying K (Fig. 1a).

The woodland-grassland model has two alternative states: woodland (T > 0.5) and grassland (T < 0.4) (Fig. 1). The system exhibits hysteresis with respect to K. If the system starts in a woodland state and K decreases below a threshold (specifically, a value of 0.77), the system abruptly transitions to a grassland state (Fig. 2d). Once the system has converged on a grassland state, returning K to values near the original threshold—above $K = 0.77$— does not return the system to a woodland state. Instead, K must exceed a second, higher threshold, to initiate a transition back to a woodland state. The model is, therefore, capable of producing multiple ecological phenomena, specifically: (1) critical transitions that result from gradual changes in an external driver, K, over time when $q > 1$ (Figs. 1a and 2d); (2) abruptly forced critical transitions, where an abrupt shift to grassland can occur if the K parameter changes abruptly and falls below a threshold (Fig. 2b), and; (3) gradually forced non-critical transitions resulting from gradual changes in an external driver, K, over time when $q = < 1$ (Figs. 1a and 2c).

Using the woodland-grassland model, we generated time series with 10,000 time steps each, that undergo four distinct types of change (Fig. 2a–d), with 100 iterations per type. 10,000 time steps is similar to the length of the Holocene, if we treat time steps as annual. Sediment cores on the order of 10,000 to 15,000 years are especially relevant to studying regime shifts during interglacial periods. When calculating resilience indicators, we typically used about 6000 time-steps (see below). Our workflow is diagramed in Fig. 3. In the first case, there is no change in carrying capacity (K), and the system remains woodland ("no change" time series, Fig. 2a). In the second case, carrying capacity declines suddenly from 1 to 0.6 at time step 6000, representing a decrease in precipitation that causes the system to transition from woodland to grassland abruptly ("abruptly forced critical transition" time series; Fig. 2b). In this case, although the system has two alternative states, the critical transition is driven by a rapid change in the extrinsic driver and there should be no detectable loss of ecological resilience prior to the regime shift. For the third case, we use the parameterization without alternative states ($q = 1$), exposed to a slow decline in carrying capacity from 1 to 0.6 beginning at time step 1000 ("gradually forced non-critical transition" time series; Fig. 2c). Finally, in the fourth case, a slow decline in carrying capacity from 1 to 0.6 beginning at time step 1000 (with $q = 5$) causes the system to undergo a critical transition from woodland to grassland around time step 6000 ("gradually forced critical transition" time series; Fig. 2d). In this case, a slow change in carrying capacity leads to an abrupt change in system state, caused by reorganization of intrinsic feedbacks; this is the only scenario for which we expect detectable losses of resilience prior to the ecological transition.

2.2. Sedimentary and sampling transformations

2.2.1. Sedimentary transformations and age-depth models

To model a long time series generated from analysis of a typical lake sediment core, age-depth models were used to (1) transform samples through time (annual proportional tree cover, generated by the woodland-grassland model) to samples in depth and (2) calculate the number of years represented per unit depth (Fig. 3). We used five representations of sedimentation processes to explore the effects of different levels of time-averaging across a core (Fig. 2e and f). First and second, we built two linear sedimentation models where mean time-averaging is constant across the record (deposition time: either 5 yrs/cm or 20 yrs/cm; Fig. 2e). In the linear model, a plot of age on the y axis versus depth on the x axis is a straight line. We incorporated the noise inherent to sediment cores by drawing the number of years per sample randomly from normal distributions with means of either 5 or 20 yrs/cm and standard deviations of 5% of the mean. Time-averaging means (5 and 20 yrs/

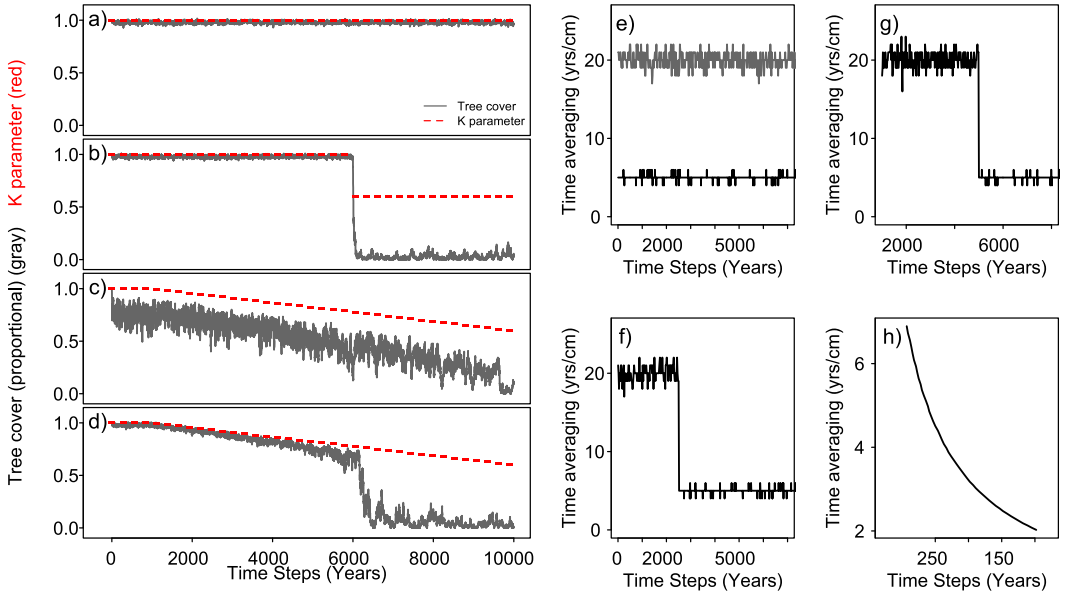

Fig. 2. Simulated ecological time series and sedimentary age-depth models. a-d) Simulated time series (gray), with corresponding changes in the K parameter (red, dashed line); a) No change; b) abruptly forced critical transition; c) gradually forced non-critical transition; d) gradually forced critical transition. e-g) Sedimentary age-depth models, illustrating in the degree of time-averaging produced by each model; e) linear age-depth model and uniform (with white noise) time-averaging (gray = 20 years/cm deposition time; black = 5 years/cm); f) Broken-stick linear age-depth model, with abrupt sedimentary regime shift from 20 years/cm to 5 years/cm at time step 2500, far from the critical transition; g) Broken-stick age model, with break-point at time step 4000, close to the critical transition; h) Exponential age model for recent (<200 years) sediment deposition (data from Taranu et al., 2018). (For interpretation of the references to color in this figure legend, the reader is referred to the Web version of this article.)

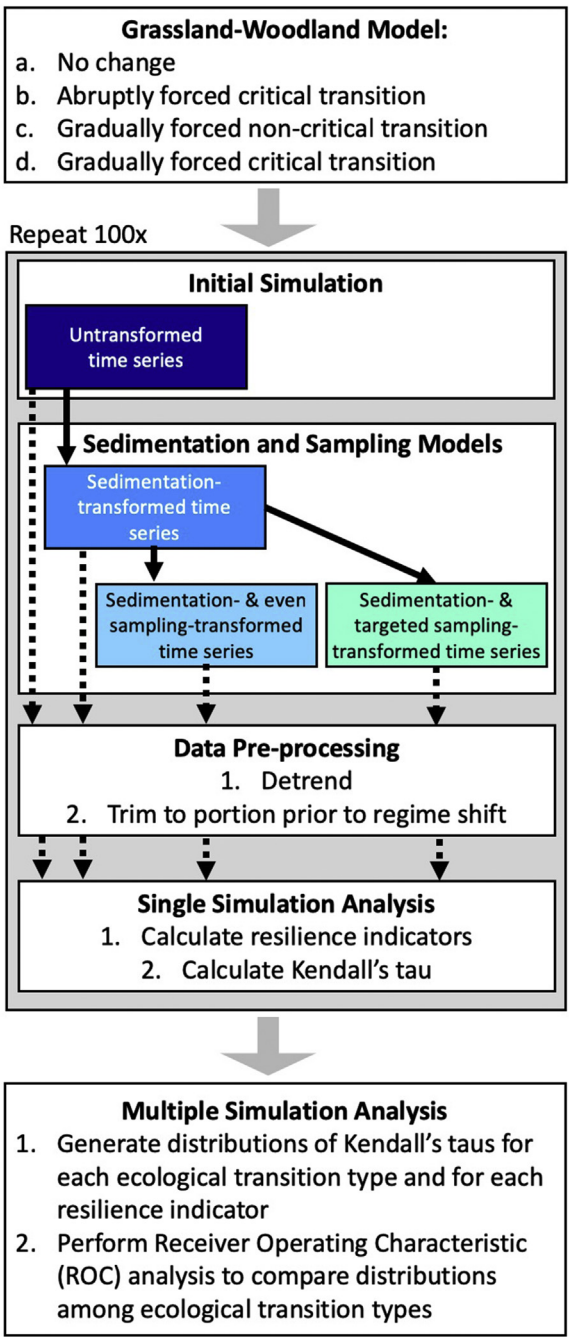

Fig. 3. Methods flow chart.

cm) are based on empirical values from 152 lacustrine sites in northeastern North America (Goring et al., 2012). We prescribe standard deviation of time-averaging to 5% of the mean, based on the observation that autocorrelation in deposition rates is high in lacustrine systems. These linear models explore the role of sample resolution in detectability of resilience indicators.

Third and fourth, we built two "broken-stick" models, representing situations when sediment deposition rates abruptly change, due to changes in lake productivity or allocthonous sediment deposition (Davis et al., 1984). Regime shifts in deposition rate have the potential to confound resilience indicators, for example by increasing standard deviation and/or autocorrelation when time-averaging decreases. In the first broken-stick model, a sedimentation regime shift from 20 yrs/cm to 5 yrs/cm is placed long in advance of the ecological regime shift (time step 2500; Fig. 2f); in the second, the same-magnitude shift in sedimentation is placed close to the ecological regime shift (time step 4000; Fig. 2g). Finally, we modeled time as an exponential function of sediment depth as a special case, intended to represent the uppermost portion of the lake sediment column where sediments are still experiencing dewatering and compression (Taranu et al., 2018) (Section 2.4; Fig. 2h).

To maintain the same number of time steps across iterations, we truncated both gradually and abruptly forced critical transition time series by identifying the time of woodland-grassland transition (generally around time step 6000) using the Cross-Entropy method for break-point detection (maximum number of break-points = 1) in the R *breakpoint* package (R Core team, 2017; Priyadarshana and Sofronov, 2016). As illustrated in Fig. 4a, we then retained 4999 time steps prior to, and 2000 time steps following the transition to grassland, producing a time series of 7000 time steps. We trimmed the no change and gradually forced non-critical transition time series to time steps 1000 (the time point at which K begins to decline in the gradually forced critical and non-critical transition time series) through 8000. This paralleled the method for gradually and abruptly forced critical transition time series in terms of maintaining time series length (7000 time steps) and the approximate location of the time series subset. Sedimentary transformations were then applied to these trimmed time series, as illustrated in Fig. 4b–d.

2.2.2. Sampling

Many paleoecological measurements are labor-intensive or costly, so discontinuous sampling designs are common (e.g. 1-cm thick volume of sediment at evenly-spaced depths). To maintain the same sample size across iterations, we built a sampling model, called even sampling, consisting of 200 1-cm samples distributed at even depth increments along the time-averaged time series (Fig. 4a and c). Note that this sampling system is evenly distributed in depth, not time, because sediment sampling usually begins before age controls are obtained and age-depth models built. We built a second sampling model, called targeted sampling, representing high-resolution sampling of intervals of interest (Fig. 3). In this model, we distributed the 200 samples such that 40% of samples (N = 80) were targeted to the 10% of the time series immediately preceding the regime shift, and the remaining 120 samples were distributed evenly across the remainder of the core (Fig. 4a and d). For the gradually forced non-critical transition and no change time series, the targeted samples were distributed between time steps 5300 and 6000 (the 10% of the time series prior to time step 6000).

2.3. Signals of critical transitions

We computed indicators of resilience loss and critical transitions for untransformed, sedimentation-, and sedimentation-and-sampling-transformed variants of each ecological time series (no change, abruptly forced critical transition, gradually forced non-critical transition, and gradually forced critical transition) (Figs. 3 and 4). Strong indications of resilience loss are expected only for the last case, but various processes may dampen signals (e.g. time-averaging, discontinuous or irregular sampling) while others may produce false positives (e.g. gradually forced non-critical transition, extrinsic abrupt changes in tree cover, abrupt changes in time-averaging) (Kéfi et al., 2013).

We used two common resilience indicators, standard deviation and autocorrelation time, to identify potential signs of critical transitions in each time series and its various transformations (Fig. 3). Autocorrelation time, τ, is a monotonic transformation of

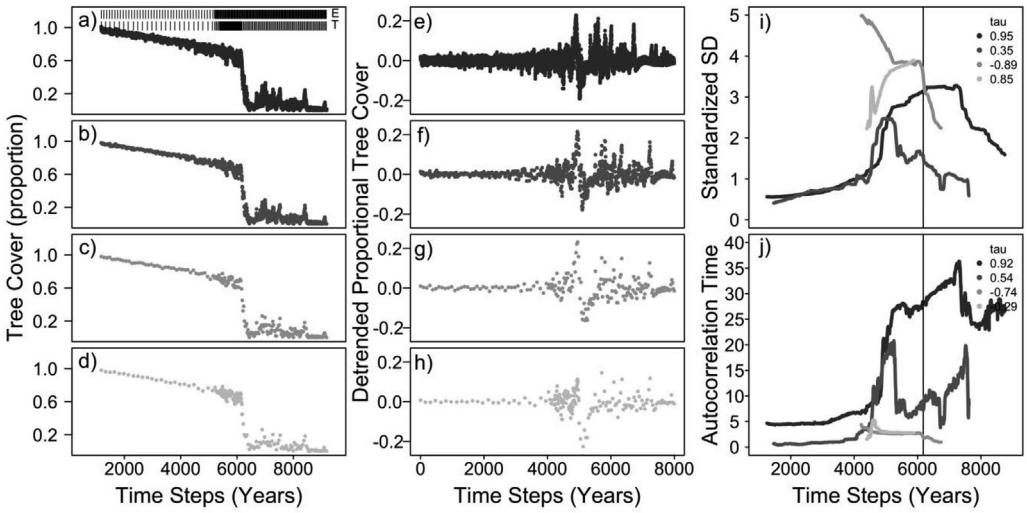

Fig. 4. Methods example: time-averaging, sampling, detrending, and resilience indicator calculation for a single simulated time series. a) Gradually forced critical transition time series generated by the woodland-grassland model and trimmed to 4999 time steps prior, and 2000 time steps subsequent to the time of transition. The labels E and T, and associated vertical tick marks, indicate even sampling and targeted sampling, respectively. In panel b), the ecological time series has been passed through a broken-stick age-depth model with break-point at time step 4000, close to the critical transition. The age-depth-transformed time series is subsampled: c) at even depth intervals; and, d) at targeted depth intervals, with 40% of samples concentrated in the 10% of the time series prior to the critical transition. Panels e–h) show detrended versions of the time series in a-d. Panels i,j) show two resilience indicators— i) standard deviation and j) autocorrelation time—calculated as rolling window statistics for each time series in panels e–h, along with Kendall's tau trend statistics. The vertical gray line in panels i,j) indicates the time of the woodland-grassland transition. Kendall's tau was calculated only for the portion of the time series prior to woodland-grassland transition time. Rolling window length was 2500, 1200, 100, and 100 samples for untransformed time series (black), sedimentation-transformed time series (dark gray), sedimentation- and even sampling-transformed time series (medium gray) and sedimentation- and targeted sampling-transformed time series (light gray), respectively.

lag-1 autocorrelation, ρ, defined as $\tau = -1/\ln(|\rho|)$ (Dai et al., 2012). Both standard deviation and autocorrelation time are expected to increase prior to a critical transition and approach infinity at the critical transition point.

Several corrections were applied during the process of estimating the indicators. First, we detrended each time series using Gaussian smoothing with a bandwidth of 310 time steps (Figs. 3 and 4e-h), determined using "Silverman's rule of thumb" (Silverman, 1986). Because the various age-depth models generate different amounts of time-averaging, the amount of time encompassed by each rolling window differs even though number of samples is held constant. To standardize for this, within each rolling window we multiplied proportional tree cover by the square root of the amount of time encompassed by the window, then calculated standard deviation on the resulting values, following the recommendation of Carstensen et al. (2013). Autocorrelation time was calculated from autoregression lag-1.

Resilience indicators were calculated for the time series prior to the woodland-grassland transition time, in rolling windows of approximately 50% of the length of the time series prior to transition, following the recommendation of Dakos et al. (2012). Window length for untransformed time series was 2500 samples, and was 50 samples for even and targeted sampled time series. Each age-depth model generates a different number of time-averaged samples and so the time series length differed after sedimentation transformation. Thus, window length varied among sedimentation-transformed time series: constant (5 yrs/cm), window length = 600 samples; constant (20 yrs/cm), window length = 150 samples; broken-stick (break-point = 2500), window length = 400 samples; broken-stick (break-point = 4000), window length = 300 samples.

We used Kendall's tau (Wilks, 1995) to quantify trends in standard deviation and autocorrelation time prior to the woodland-grassland transition time (Dakos et al., 2012). Fig. 4i and j illustrate example trajectories for these indicators and Kendall's tau values for each transformation of a single time series. Kendall's tau is a non-parametric trend statistic, ranging from −1 (negative trend) to 1 (positive trend). Kendall's tau is commonly used to assess whether trends in resilience metrics are significant and hence indicative of a critical transition (Dakos et al., 2012). We generated histograms of Kendall's tau values (Fig. 3), computed summary statistics, and calculated the 95% confidence intervals for each distribution (Figs. 5–8, Appendix B and C).

We used receiver operating characteristic (ROC) analysis (Gavin et al., 2003) to assess the diagnostic ability of Kendall's tau for determining whether a given time series contains signals of a critical transition (Fig. 3). ROC analysis is a method for assessing the overall diagnostic value of a test metric and the optimal decision threshold, given two populations with overlapping values of the metric. Here, Kendall's tau is the test metric and we compared the time series we expected to have true positives for resilience indicators—the gradually forced critical transition—to the other three types of ecological transition as a group, and to each scenario individually. The optimal decision threshold identifies the Kendall's tau value (Kt') that jointly maximizes the fraction of observed Kendall's taus less than *Kt'* that are truly from gradually forced critical transition time series (the true positive fraction, TPF) and the fraction of Kendall's tau values greater than *Kt'* that are truly not from gradually forced critical transition time series (the true negative fraction, TNF). A plot of TPF versus 1-TNF over the range of *Kt'* values and its area under the curve (AUC) measures the overall ability of Kendall's tau to discriminate gradually forced critical transitions from the others. AUC ranges between 0.5, meaning the distributions are completely overlapping, and 1, meaning the distributions are completely separated. We created a modified version of the *ROC* function from the R *analogue* package (Simpson, 2007; Simpson and Oksanen, 2016).

2.4. Exponential model and short cores

Exponential age-depth models are often appropriate for the top of sediment sequences, where sediments are still experiencing

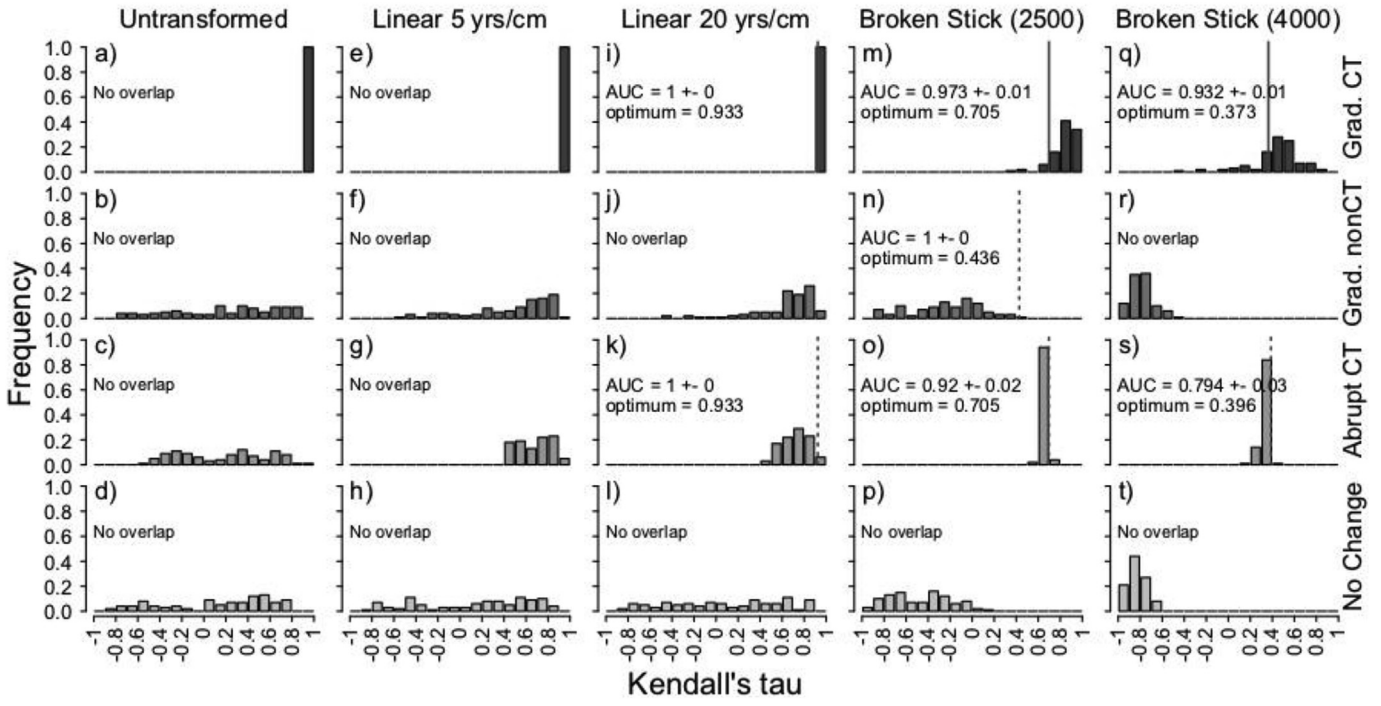

Fig. 5. Effects of sedimentary transformations on the resilience indicator signals and diagnostics, shown as histograms of Kendall's tau values for standard deviation, for untransformed and transformed time series. a-d) Untransformed time series, for a) the gradually forced critical transition, b) gradually forced non-critical transition, c) abruptly forced critical transition, and d) no change; e-h) Time series transformed by linear sedimentation and uniform time-averaging (deposition time: 5 yrs/cm); i-l) Time series transformed by linear sedimentation and uniform (20 yrs/cm) time-averaging; m-p) Time series transformed by broken-stick age model (with abrupt sedimentary regime shift far from the critical transition); q-t) Time series transformed with broken-stick age model (with sedimentary regime shift close to critical transition). AUC is the area under the curve from ROC analysis, ± the standard error; where no standard error is shown, the gradually forced critical transition Kendall's tau distribution is non-overlapping with the distribution against which it is being compared. Solid gray vertical lines show the optimum decision threshold from ROC analysis when comparing gradually forced critical transition to all other ecological transition types together. Dashed gray vertical lines show optimum decision thresholds for gradually forced critical transition versus each of the three ecological transitions individually.

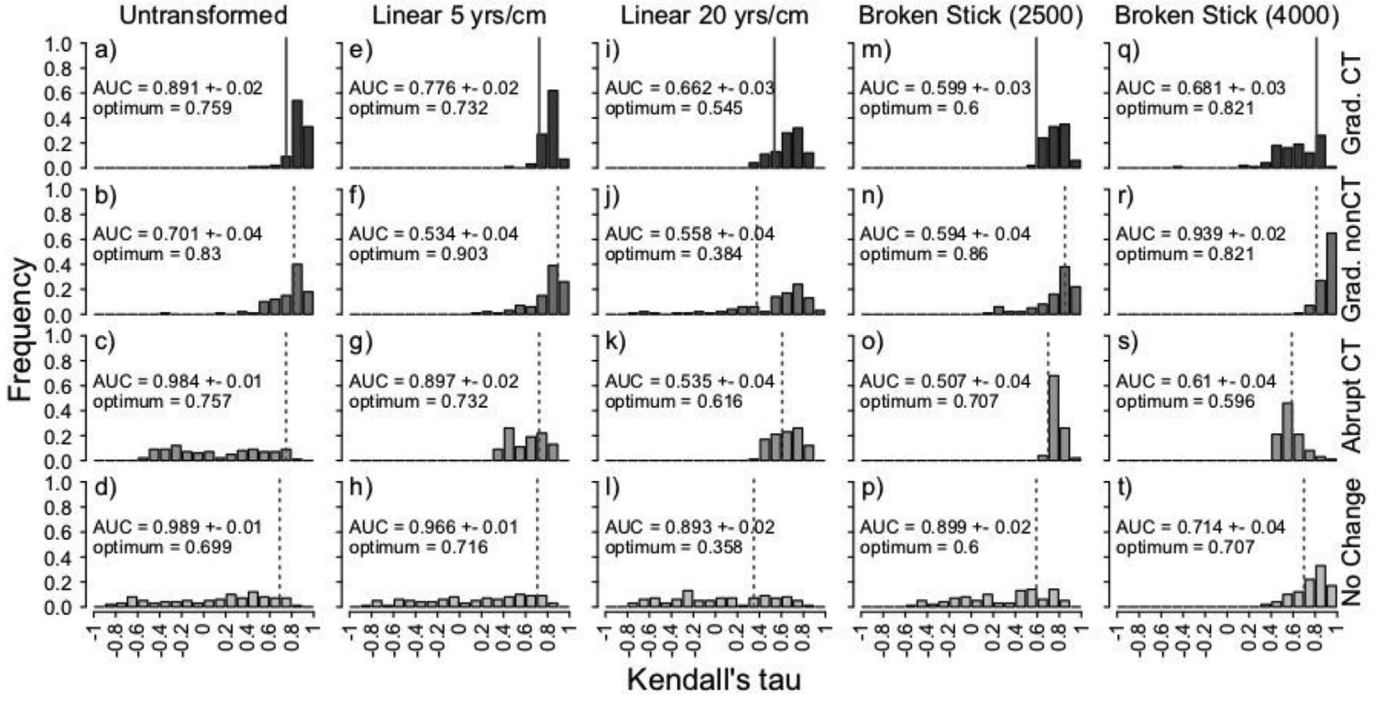

Fig. 6. Effects of sedimentary transformations on resilience indicators and diagnostics, shown as Kendall's tau values for autocorrelation time, for untransformed and age-depth transformed time series. Figure design follows Fig. 5.

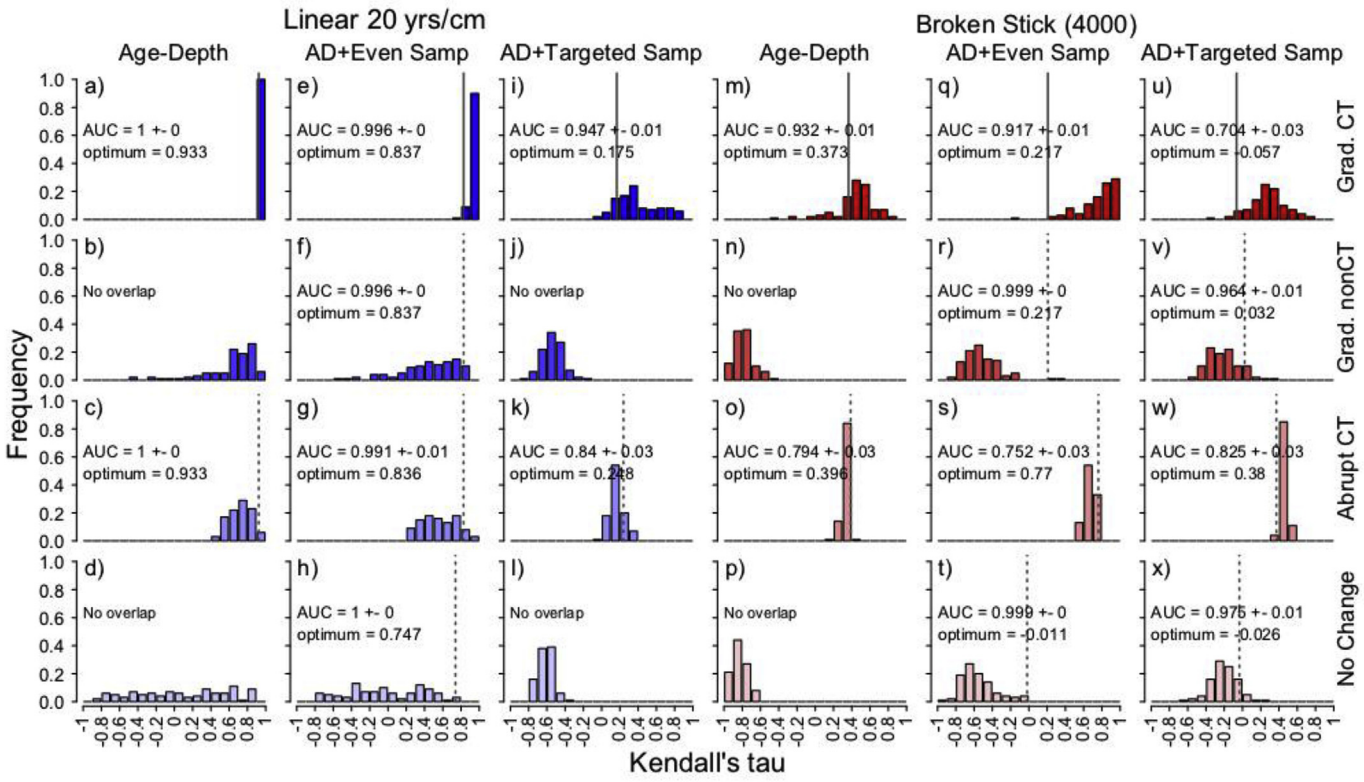

Fig. 7. Effects of time-averaging, sampling, and sedimentation regime shifts on standard deviation as a resilience indicators and diagnostics for transformed time series. Panels a–d): Time-averaging only (linear sedimentation, deposition time: 20 years/cm) for time series with a a) gradually forced critical transition, b) gradually forced non-critical transition, c) abruptly forced critical transition, and d) no change. Panels e–h: time-averaging (20 years/cm) with subsampling at even depth intervals. Panels i–l): time-averaging (20 years/cm) with targeted subsampling. Panels m–x): panel arrangement as for panels a–l), but for the broken-stick age-depth model, with an abrupt sedimentary regime shift at time step 4000, close to the ecological critical transition. Figure design follows Fig. 5.

dewatering and compression. Short cores from the top of sediment columns are of particular interest to researchers studying recent and anthropogenic impacts on ecosystems over the past several decades to centuries.

We applied an exponential age-depth relationship to simulated short cores. In the exponential model, a plot of age on the y axis versus depth on the x axis is an exponential function of depth, with parameters fitted by Taranu et al. (2018) to empirical data from 108 sediment cores from lakes across the Temperate and Subarctic zones, spanning ~200 calendar yrs BP to the present (Fig. 2h) (Taranu et al., 2018). The model uses a fitted linear relationship of inverse sedimentation rate (cm/year) and age of a core slice. We assumed an intercept of 2 and slope of 0.025, corresponding to intermediate levels of sediment compression (Taranu et al., 2018).

To simulate short cores, we used the woodland-grassland model to generate time series of 300 time steps. For gradually and abruptly forced critical transitions, we trimmed to 149 time steps prior to the woodland-grassland transition and 50 time steps following. For no change and gradually forced non-critical transition time series, we used time steps 60 through 210. For sampling, we distributed 25 1-cm samples along the time-averaged time series. Window length for resilience indicator analysis was 150 for untransformed time series, 20 for sedimentation-transformed, and 10 for both even and targeted sampling-transformed time series.

2.5. *Real-world example: assessing observed regime shifts in forest-grassland conversion at Steel Lake, Minnesota, USA*

To illustrate how this approach might be used to assess whether a real-world system shows signals of resilience loss prior to a regime shift, we analyzed a record of forest-to-prairie conversion at Steel Lake, Minnesota (Nelson and Hu, 2008; Williams et al., 2009). Steel Lake is an iconic record of early Holocene deforestation in the Great Plains with strong dating control (26 radiocarbon dates), multiple paleoecological and paleoenvironmental proxies, and relatively high temporal resolution (mean resolution = ~103 years between samples). Gradual aridification began at Steel Lake around 9400 yrs BP, followed by a sharp increase in aridity around 8000 yrs BP, based on changing mineral composition in the sediments and other indicators (Nelson and Hu, 2008). Woody cover first gradually declined with aridification, then rapidly dropped from around 60% at ~8200 yrs BP to less than 40% at 8000 yrs BP (Williams et al., 2009). These climatic and vegetation changes were accompanied by changes in fire activity (Nelson et al., 2004; Nelson and Hu, 2008).

We assessed whether the shift to prairie was associated with resilience loss indicative of a critical transition driven by a gradually drying climate. We focused our analysis of resilience indicators on the early Holocene forested period (11,100 to 8200 yrs BP) when % woody cover was greater than 50%. We also performed a second analysis in which search for resilience signals was limited to the time period with independent evidence of aridification (9400–8200 yrs BP) (Fig. 9a). As in the simulations, we used breakpoint analysis to estimate the time of the forest-prairie regime shift at Steel Lake, detrended the time series using Gaussian smoothing, and calculated standard deviation in rolling windows set to 50% of the length of the Steel Lake record prior to the regime shift: either 17 (full dataset) or 10 samples (period of aridification only). We then calculated Kendall's tau for standard deviation prior to the regime shift. This empirical estimate was compared to 100

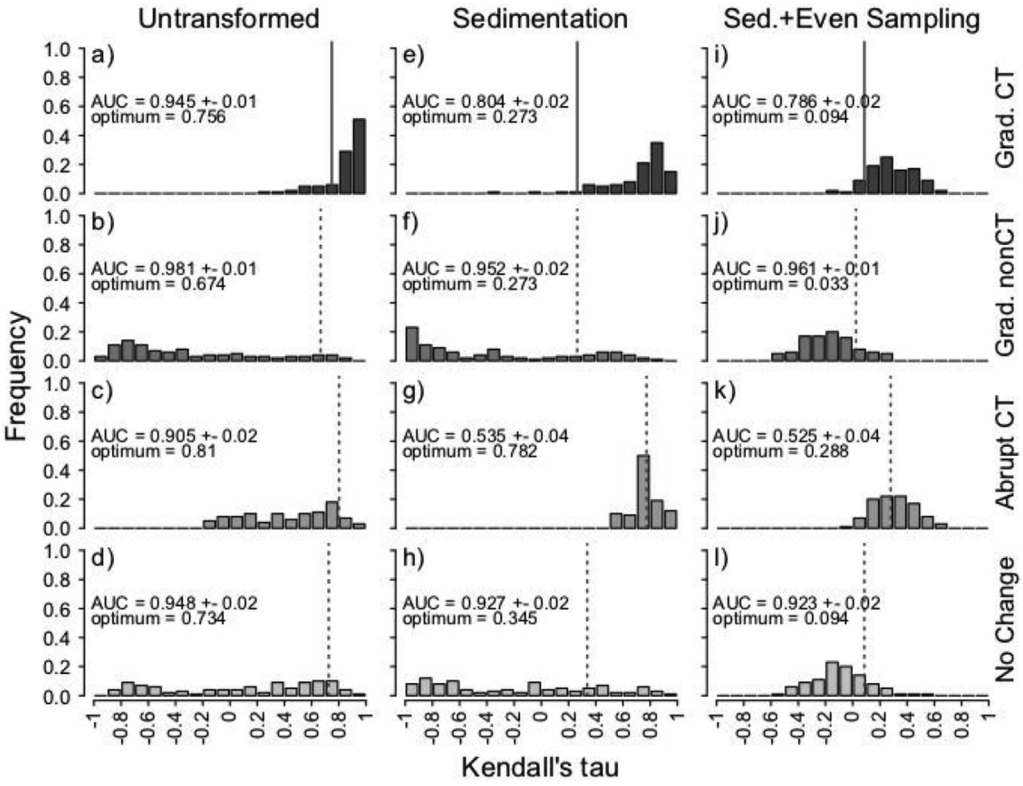

Fig. 8. Effect of exponential sedimentation transformation on standard deviation as a resilience indicators and diagnostics for transformed time series. Kendall's tau distributions of standard deviations for a-d) untransformed, e-h) sedimentation-transformed, and i-l) sedimentation and even-sampling-transformed time series. a,e,i) a gradually forced critical transition, b,f,j) gradually forced non-critical transition, c,g,k) abruptly forced critical transition, and d,h,l) no change time series.

gradually forced and 100 abruptly forced critical transitions simulated with the woodland-grassland model, using the same model parameters as previously described. We trimmed the simulated time series to either 2930 (full dataset) or 1176 years (aridification period only) prior to the simulated regime shift to match the Steel Lake record. We matched the simulated sedimentation model to observed Steel Lake sediment deposition rates and sampling. We calculated standard deviation for our simulations in rolling windows of 17 (full dataset) or 10 samples (period of aridification only), calculated Kendall's taus, and used ROC analysis to compare Kendall's tau distributions for simulated gradually and abruptly forced critical transitions. We also tested the effect of doubling the number of samples, to determine whether increasing temporal resolution has the potential to improve ROC discriminant ability.

3. Results

3.1. Untransformed time series

3.1.1. Standard deviation

Prior to transformation, gradually forced critical transitions were always distinguishable from other ecological transition types based on standard deviation. Before sedimentation and sampling, gradually forced critical transitions had Kendall's taus for standard deviation (SD-Kt) which were higher than, and non-overlapping with, all other ecological transition types (Fig. 5a–d and Appendix B). This indicates that temporal variability consistently increased leading up to a critical transition resulting from a gradual change in an external driver, as expected from theory (e.g. Scheffer et al., 2015). The SD-Kt distributions for abruptly forced critical transitions, gradually forced non-critical transitions, and no change time series overlapped considerably with one another (Fig. 5b–d and Appendix B).

3.1.2. Autocorrelation time

The Kendall's tau (AC-Kt) distributions of autocorrelation time for gradually forced critical and non-critical transitions were very similar (AUC = 0.70) (Fig. 6a and b). However, gradually forced critical transitions were easily distinguished from abruptly forced critical transitions and no change time series based on AC-Kt distributions (AUC values > 0.98). In comparing gradually forced critical transitions to other ecological transitions as a group, discriminant ability was fairly high (AUC = 0.89) and the Kendall's tau optimum decision threshold was 0.76. AC-Kt distributions for no change and abruptly forced critical transitions were strongly overlapping with one another (Fig. 6c and d, and Appendix C).

3.2. Constant mean time-averaging

3.2.1. Standard deviation

Standard deviation remained a clear indicator of gradually forced critical transitions even with time-averaging. Constant time-averaging had little impact on the SD-Kt distribution for gradually forced critical transitions and no change time series, but shifted to higher values the distributions for gradually forced non-critical transitions and abruptly forced critical transitions (Fig. 5e-l and Appendix B). As a result, gradually forced non-critical transitions, abruptly forced critical transitions, and no change time series developed overlapping SD-Kt distributions. SD-Kt values for gradually forced critical transitions were higher than, and non-overlapping with SD-Kt distributions for the other three ecological transitions when time-averaging was 5 yrs/cm. When time-

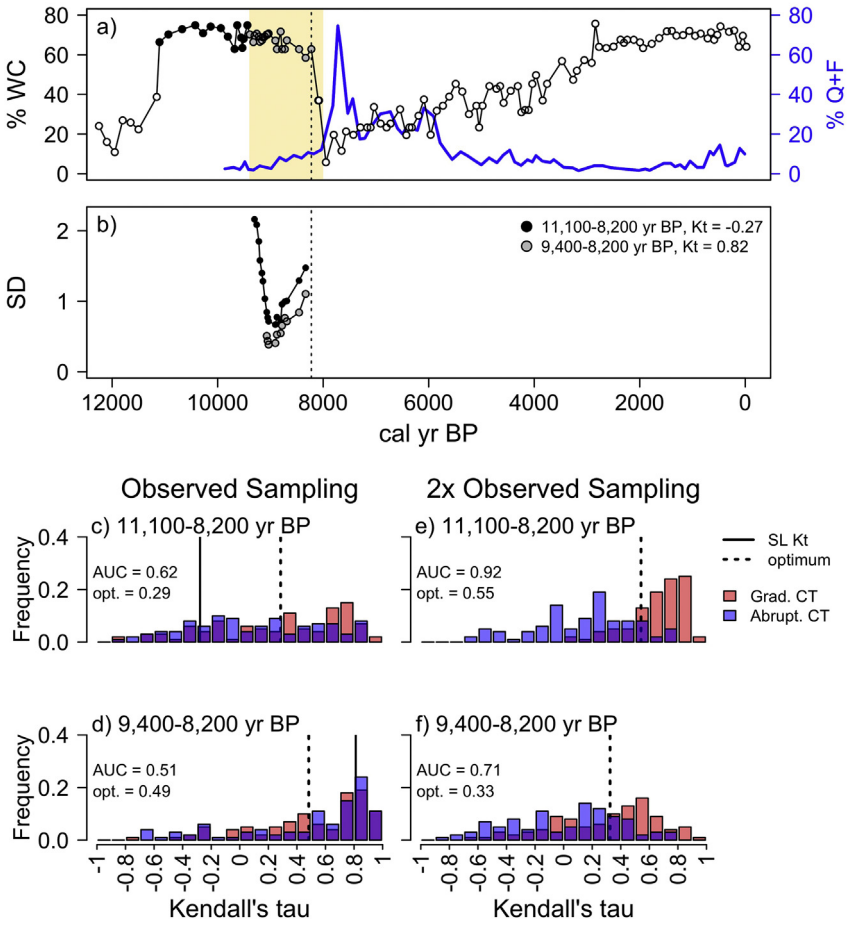

Fig. 9. Regime shift at Steel Lake. a) Estimated % woody cover (%WC; black line, open and filled points) and quartz + feldspars (Q + F; blue line) at Steel Lake. Filled points are %WC data used for resilience indicator analyses; gray points are %WC samples that correspond to the timing of gradual aridification. Yellow shading shows the time period of gradual aridification. b) Standard deviation (SD) of Steel Lake %WC for the full record (all filled points in panel a)) and for the period of aridification alone (gray filled points in panel a)); Kt = Kendall's tau. Black dashed lines in a) and b) show the time of regime shift. c,d,e,f): Distribution of standard deviation Kendall's tau values for simulated gradually forced critical transitions (red bars) and simulated abruptly forced critical transitions (blue bars), with the same sedimentation model and time of regime shift as at Steel Lake, and c,d) the same sample resolution, or, e,f) double the sample resolution as Steel Lake. SL Kt = Kendall's tau for Steel lake standard deviation (black vertical line); optimum decision threshold from ROC analysis of simulated data (dashed black line). (%WC data come from Williams et al. (2009) and Nelson et al. (2004); quartz + feldspars data come from Nelson and Hu (2008)). (For interpretation of the references to color in this figure legend, the reader is referred to the Web version of this article.)

averaging was 20 yrs/cm, the SD-Kt distributions of gradually forced critical transitions are significantly different from the other three times series types (non-overlapping 95% CIs, Appendix B), and there is either no overlap or AUCs = 1 (Fig. 5i and k), meaning essentially perfect discrimination.

3.2.2. Autocorrelation time

For time-averaging of either 5 or 20 yrs/cm, autocorrelation time was sensitive to time-averaging and became ineffective as an indicator of resilience loss and of gradually forced critical transitions. Constant mean time-averaging drove the AC-Kt distributions for gradually forced critical and non-critical transitions downward relative to untransformed time series, while also shifting abruptly forced critical transitions and no change distributions to higher values (Fig. 6e-l and Appendix C), generating strong overlap among all types of ecological transitions (Appendix C). Low AUC values (<0.6) indicated low discrimination between gradually forced critical and non-critical transitions for this resilience indicator (Fig. 6f and j). This in turn drove low discrimination between gradually forced critical transitions and all other transitions (AUCs = 0.77 and 0.66 for 5 yrs/cm and 20 yrs/cm age models, respectively (Fig. 6e and i). The separation between AC-Kt distributions for gradually and abruptly forced critical transitions decreased when time-averaging increased (Fig. 6g and k). AC-Kt distributions for gradually forced critical transitions and no change time series had the least overlap (Fig. 6h and l), resulting in relatively high AUC values (AUCs ~0.9).

3.3. Broken-stick time-averaging

The directions of change in SD-Kt and AC-Kt distributions were similar between broken-stick age-depth models, but were more severe for break-points close to the regime shift (time step 4000; Fig. 5q–t and 6q-t) versus those that were far from the transition (time step 2500; Fig. 5m–p and 6m-p) (Appendix C).

3.3.1. Standard deviation

When a broken-stick age model was applied, the SD-Kt distributions of gradually forced critical transitions were still easily discriminated from other time series types, but there was more overlap between gradually and abruptly forced critical transitions than under constant time-averaging (Fig. 5). Broken-stick age models shifted upward and reduced the range of SD-Kt values for abruptly forced critical transitions, but shifted downward the SD-Kt

distributions for all other ecological transitions (Fig. 5m–t and Appendix B). Nevertheless, there was very low overlap between SD-Kt distributions of gradually forced critical and both gradually forced non-critical transitions and no change time series. Discrimination was high under both broken-stick age models (all AUCs > ~0.79, or no overlap), and the optimum discriminant threshold was low for gradually versus abruptly forced critical transitions (threshold = 0.70 and 0.40 for break-points at time step 2500 and 4000, respectively). Hence, a wide range of SD-Kt values were indicative of a gradually forced critical transition.

3.3.2. Autocorrelation time

As with constant time-averaging, broken-stick age models essentially eliminated any potential for using autocorrelation time to distinguish gradually forced critical transitions from the three other ecological transition types. AC-Kt distributions shifted slightly downward for gradually forced critical transitions and upward for the other ecological transition types (Fig. 6m–t and Appendix C). In general, AUC values demonstrated low discrimination between gradually forced critical transitions versus both gradually forced non-critical transitions and abruptly forced critical transitions (Fig. 6n, o, r, and s) under either broken-stick age model. An apparent exception was the comparison of gradually forced critical and non-critical transitions with the break-point at time step 4000, where the AUC values suggested high discrimination (AUC = 0.94). However, this is because gradually forced non-critical transitions actually had overall *higher* AC-Kt values than gradually forced critical transitions, so while the distributions could be distinguished from one another with high confidence, the utility of AC-Kts as indicators of gradually forced critical transitions was questionable. The same held true for the comparison of gradually forced critical transitions and no change time series with the break-point at time step 4000.

Given the poor performance of autocorrelation time (AC-Kt) as a diagnostic indicator of resilience loss before critical transitions, subsequent analyses focus only on the Kendall's tau of standard deviation (SD-Kt).

3.4. Sensitivity to discontinuous sampling

Relative to continuously sampled sedimentation-transformed time series, discrimination of gradually forced critical transition SD-Kt distributions was only slightly diminished when sampling was discontinuous—regardless of whether sampling was evenly-space or targeted, and whether time-averaging was constant. This is because sampling drives all SD-Kt distributions lower, but the effect was less extreme for gradually forced critical transitions. For constant time-averaging, even sampling better discriminates SD-Kt distributions of gradually forced critical transitions versus abruptly forced critical transitions than did targeted sampling (Fig. 7g and k, Appendix B). In contrast, targeted sampling improved discrimination of gradually forced critical transition SD-Kt distributions versus gradually forced non-critical transitions or no change time series (Fig. 7f, j, h, and l, and Appendix B).

For broken-stick age models, even sampling caused SD-Kt distributions to increase for all four time series types (relative to the SD-Kt distributions of continuous, sedimentation-transformed time series), while also decreasing discrimination of gradually forced critical transitions across the board (Fig. 7m–x and Appendix B). Targeted sampling further reduced discriminant ability, i.e. relative to even sampling when the age model was broken-stick (Fig. 7u–x and Appendix B).

3.5. Exponential age-depth model and short cores

The exponential age-depth model (Fig. 2h) strongly and adversely affected the ability of SD-Kt (and AC-Kt; Appendix C) distributions to correctly capture signals of resilience loss. The 95% confidence intervals for SD-Kts overlapped among all four time series types after exponential transformation, particularly distributions for gradually and abruptly forced critical transitions (Fig. 8). The SD-Kt distributions for gradually forced critical transitions, gradually forced non-critical transitions, and no change time series shifted downward, whereas the distributions for abruptly forced critical transitions moved upward and their range narrowed (Fig. 8e–h and Appendix B). Sampling reversed these trends for all ecological transition types except gradually forced critical transitions (Fig. 8i-l). Separation between gradually forced critical transitions and both gradually forced non-critical transitions and no change time series remained reasonably high (AUC > 0.92) after age-depth transformation (Fig. 8e, f, and h) and even sampling (Fig. 8i, j, and l). However, there was high overlap and low discrimination between SD-Kt distributions for gradually and abruptly forced critical transitions after any time time-averaging and sampling (AUCs < 0.53; Fig. 8e, g, i, and k). Targeted sampling generated strong overlap and low discrimination (all AUCs < 0.76) among all ecological transitions types (Appendix B).

3.6. Testing for critical transitions in empirical data: Steel Lake

Break-point analysis of % WC identified a regime shift at 8224 yrs BP. For the full period of high woody cover from 11,100 to 8200 yrs BP, standard deviation initially declined, then increased (Kendall's tau = −0.27; Fig. 9b). However, during the period of increasing aridity (9400–8200 yrs BP), standard deviation increased steadily (Kendall's tau = 0.82; Fig. 9b).

Simulated gradually and abruptly forced critical transitions with the same age model, sampling, and time of regime shift as Steel Lake produced overlapping and only weakly informative SD-Kt distributions (AUC = 0.65 for 11,100–8200 yrs BP; AUC = 0.62 for 9400–8200 yrs BP) (Fig. 9c and d). When the full period of early Holocene tree cover was analyzed, the optimum discriminant threshold for the simulations was 0.29, which was greater than the observed Kendall's tau (−0.27), suggesting that the empirical data failed to pass the simulated threshold used to discriminate gradually forced critical transitions from other regime shifts. However, when only the period of known aridification was analyzed, the observed Kendall's tau (0.82) exceeded the simulated optimum discriminant threshold of 0.49, suggesting a signal of resilience loss for that time period (Fig. 9c and d). In additional simulations (Fig. 9e and f), a doubling of sampling density increased the potential discriminant ability (AUC = 0.92 for the full period, and AUC = 0.71 for the aridification period).

4. Discussion

Regime shifts can alter ecosystems unexpectedly, and these changes are likely to become more frequent as anthropogenic global change progresses (Barnosky et al., 2012; Steffen et al., 2015a). Forecasting which systems are resilient and which are approaching thresholds (Lenton et al., 2008) has clear advantages (Dietze et al., 2018), allowing us to potentially prevent, mitigate, or adapt to large ecological shifts. Long ecological time series, particularly those from sedimentary archives, are rich in signals of past regime shifts, but inferring their causes is difficult (Williams et al., 2011). For instance, do these regime shifts represent critical transitions that would be difficult to reverse contemporaneously, or instances where drivers merely changed abruptly? Resilience

indicators are a promising avenue for identifying gradually forced critical transitions, but application to paleoecological time series are often hindered by time-averaging, missing data, and other irregularities. Our results are promising, in that they show that some resilience indicators (particularly standard deviation) retain their signal under several common time-averaging and sampling scenarios associated with paleoecological sedimentary time series. However, some scenarios, especially those associated with recent sediment records, distorted the data too much to detect resilience indicators.

Standard deviation is relatively robust to time-averaging and discontinuous sampling and is a broadly effective indicator of gradually forced critical transitions in paleoecological records when age-depth relationships are linear and time-averaging varies around a constant mean. Linear sedimentation regimes are common in large sections of many lake sediment records (e.g. Steel Lake, Goring et al., 2012) and so resilience indicators that measure changes in variance may well be able to detect signals of critical transitions. This holds true even when there is noise around the mean time-averaging, provided that the amount of time per sample is accounted for (Carstensen et al., 2013). Standard deviation indicators are even robust to abrupt changes in sedimentation regime, provided that any break-points in time-averaging occur relatively far before the regime shift. The robust performance of standard deviation in our study is consistent with other studies from a range of systems (e.g., Carpenter and Brock, 2006; Dakos et al., 2008; Carpenter et al., 2011; Dai et al., 2012; Dakos et al., 2012; Veraart et al., 2012; Cimatoribus et al., 2013; Pace et al., 2017; Wilkinson et al., 2018; but see Hastings and Wysham, 2010). Frossard et al. (2015) also used simulated critical transitions to test various resilience indicators at constant levels of time-averaging and found that standard deviation was robust to all tested levels of time-averaging. Indeed, uniform time-averaging can sharpen signals of resilience changes by dampening short-term trends, like inter-annual variability (Lenton et al., 2012).

Autocorrelation time is sensitive to critical transitions in theory and some simulation models and experiments (Dai et al., 2012; Scheffer et al., 2015). However, in contrast to standard deviation, signals of increasing autocorrelation time prior to critical transitions are severely degraded by sedimentation and sampling transformations in our study. Further, the performance of autocorrelation time worsens when time-averaging increases (Frossard et al., 2015), and sedimentation and sampling processes intrinsically generate autocorrelation that is independent of ecological processes. It may be possible to model the autocorrelation of these processes and to disentangle them from ecological autocorrelation, but we did not attempt that here. Other studies have found that variability is a better indicator of impending, gradually forced critical transitions than autocorrelation (e.g., Belle et al., 2017; Chen et al., 2018; Peretti and Munch, 2012; model review: Boettiger et al., 2013).

Ditlevsen and Johnsen (2010) argue that critical transitions can be inferred only when increases in *both* variance and autocorrelation are observed. Our analyses highlight the difficulty of confidently detecting both resilience indicators in sedimentary archives characterized by time-averaging and discontinuous sampling. Prior to taphonomic transformation, our simulations of gradually forced critical transitions show increases in variance and autocorrelation. After passing these simulated critical transitions through filters common in sedimentary records, we have shown that detecting increases in autocorrelation is extremely uncommon in these datasets. Thus, even if a true critical transition took place, a sedimentologically altered dataset is unlikely to meet the criteria advocated by Ditlevsen and Johnsen (2010). The converse is also true: sedimentary processes can generate autocorrelation signals in time series that did *not* undergo a critical transitions, potentially leading to false positives. Autocorrelation is therefore an unreliable indicator of critical transitions for many of the data alterations covered here.

These analyses also highlight the difficulty of using simple metrics of resilience loss in sediments characterized by exponential age-depth relationships. Unfortunately, approximately exponential relationships are common in the uppermost portion of lake sediments, which are often targeted for short cores seeking to study environmental and anthropogenic perturbations to lake ecosystems over the last several decades to centuries (e.g., Smol et al., 2005; Wang et al., 2014; Bunting et al., 2016; Belle et al., 2017). The exponential age-depth models produce such strong internal variations in time-averaging and sample spacing that they alter the standard deviation and autocorrelation time signatures to the point that these indicators are not informative.

These analyses further suggest that standard thresholds for detecting resilience loss using the indicators evaluated here will be too conservative when applied to time series with time-averaging and discontinuous sampling (i.e. they will fail to detect actual resilience loss and critical transitions) because these effects tend to weaken signals of resilience loss. Note that the ROC results and discriminant threshold values established here are sensitive to the choice of ecological system model and of sedimentation and sampling model, and so the thresholds reported here cannot be applied to other systems.

However, this modeling framework could be readily adapted and modified to generate null models for other systems, and could be used to test various sampling designs to determine what sampling frequency would be adequate so long as the user has a model of the ecological system of interest (analogous to the woodland-grassland model used here) and knowledge of the sedimentation or time-averaging regime. This approach can also be used to test sampling designs intended to study the resilience of systems. The Steel Lake example illustrates how to apply actual deposition rates and sampling points from a site of interest to simulations to generate a null model, and then to compare the observed regime shift to the null. Although we have focused on records with single regime shifts, our methods could be applied to time series with multiple regime shifts provided there are enough data between events to measure resilience.

In the case of Steel Lake, the increasing standard deviation from 9400–8200 yrs BP is consistent with loss of resilience associated with a gradual trend towards increasing aridity (Nelson and Hu, 2008) and a regime shift from woodland to a grassland state. In contrast, the trend in standard deviation from 11,100–8200 yrs BP is inconsistent with a gradually forced critical transition. This demonstrates that variance in ecological time series can change for a variety of reasons, that simple measures of resilience loss are not strongly diagnostic on their own, and that the addition of an independent climate proxy provides important complementary evidence. However, we caution that the grassland-woodland model has not been formally parameterized to represent vegetation dynamics at Steel Lake. Instead, this example serves to illustrate a possible method rather than to draw conclusions about Steel Lake specifically. Next steps could include a closer parameterization of the model, greater sampling frequency, and/or further development of the driver proxies (e.g. aridity) that remain critical for diagnosing the cause of regime shifts (Ratajczak et al., 2018).

Recent analyses of paleolimnological surrogates for lake eutrophication show that state-space models are effective for identifying gradually forced critical transitions in datasets with exponential time-averaging (Taranu et al., 2018). State-space modeling can also help develop a deeper understanding of mechanisms that underlie observed regime shifts (e.g Einarsson et al., 2016).

While critical slowing down is frequently documented in model simulations, many common ecological phenomena can make critical slowing down less likely in real-world systems. For instance, when environmental noise is large, the system can be thrown into a different state long before a bifurcation point (Thomas et al., 2015), although the system will not remain in the new state unless its resilience is higher than in the previous state. Additionally, if the rate of driver change is much faster than the rate of state change—for example if the life-cycle of the dominant organism is long relative to the driver change—then critical slowing down will not be reflected in the system state (Bestelmeyer et al., 2011). Furthermore, the resolution of the time series may be mismatched to the rates of ecological or environmental change (Thomas, 2016): increasing autocorrelation may not be observable if the resolution of the time series is coarser than the resolution of biological events. Livina and Lenton (2007) suggest that, in order to detect a critical transition in a given time series, the dataset must be an order of magnitude longer than the transition time, and the resolution must be an order of magnitude higher: empirical datasets of this length and sample resolution require high-throughput techniques. Critical slowing down and statistical indicators can also precede non-critical transitions (Kéfi et al., 2013) and so studies should also consider other models that can produce signs of critical slowing down (Boettiger et al., 2013).

5. Conclusions

The results presented here suggest that long ecological time series from sedimentary archives have promise for assessing resilience preceding gradually forced critical transitions in many circumstances, although cautions remain. The large and growing number of these records, archived in public repositories, such as NOAA-NCEI or the Neotoma Paleoecology Database, provide a wealth of information about past regime shifts and driver-state relationships across a range of systems and environments, including combinations of biotic and abiotic variables that are not currently represented. The robustness of standard deviation as a resilience indicator is encouraging, but more work is needed to develop and test other resilience indicators that are robust to sedimentary transformations. One promising avenue forward for future diagnostic studies is to develop process-based null models such as the one shown here, against which time series from empirical datasets can be compared to test hypotheses about the mechanism of regime shift, or to refine and increase the power of sampling designs. These approaches can be readily adapted to other long ecological time series extracted from sedimentary archives, including time series with multiple change points.

Declarations of interest

None.

Data accessibility

Code used in this study can be found at https://github.com/allisonstegner/PaleoResilience. Steel Lake paleoclimatic data is available from the Neotoma Paleoecology Database.

Funding

Funding for this work, and support for MAS, comes from the UW2020 initiative, underwritten by the University of Wisconsin Alumni Research Foundation. ZR was supported by the NSF (DBI-1402033) and Joint Fire Science Program (grant # 16-3-01-04). SRC was supported by NSF awards (DEB-1440297, DEB-1455461, and DEB-1754712). JWW was partially supported by NSF awards (DEB-1353896 and EAR- 1550707).

CRediT authorship contribution statement

M. Allison Stegner: Conceptualization, Methodology, Software, Validation, Formal analysis, Investigation, Data curation, Writing - original draft, Writing - review & editing. **Zak Ratajczak:** Conceptualization, Methodology, Software, Validation, Writing - review & editing. **Stephen R. Carpenter:** Conceptualization, Methodology, Writing - review & editing, Funding acquisition. **John W. Williams:** Conceptualization, Methodology, Resources, Writing - review & editing, Supervision, Funding acquisition.

Acknowledgements

Thanks to the University of Wisconsin-Madison, Abrupt Change in Ecological Systems group, Williams Lab, Hotchkiss Lab, and T. Spanbauer for helpful discussion. We thank D. Nelson for providing Steel Lake paleoclimatic data. SRC thanks Z. Taranu for extensive discussion of these ideas.

Appendix A. Supplementary data

Supplementary data to this article can be found online at https://doi.org/10.1016/j.quascirev.2019.01.009.

References

Abades, S.R., Gaxiola, A., Marquet, P.A., 2014. Fire, percolation thresholds and the savanna forest transitions: a neutral model approach. J. Ecol. 102 (6), 1386–1393.
Allen, C.D., Breshears, D.D., 1998. Drought-induced shift in a forsest-woodland ecotone: rapid landscape response to climate variation. Proc. Natl. Acad. Sci. Unit. States Am. 95, 14839–14842.
Anderies, J.M., Janssen, M.A., Walker, B.H., 2002. Grazing management, resilience, and the dynamics of a fire-driven rangeland system. Ecosystems 5 (1), 23–44.
Barger, N.N., Archer, S.R., Campbell, J.L., Huan, C., Morton, J.A., Knapp, A.K., 2011. Woody plant proliferation in North American drylands: a synthesis of impacts on ecosystem carbon balance. J. Geophys. Res. 116, G00K07.
Barnosky, A.D., Hadly, E.A., Bascompte, J., Berlow, E.L., Brown, J.H., Fortelius, M., Getz, W.M., Harte, J., Hastings, A., Marquet, P.A., Martinez, N.D., Mooers, A., Roopnarine, P., Vermeij, G., Williams, J.W., Gillespie, R., Kitzes, J., Marshall, C., Matzke, N., Mindell, D.P., Revilla, E., Smith, A.B., 2012. Approaching a state shift in Earth's biosphere. Nature 486, 52–58.
Beck, K.K., Fletcher, M.-S., Gadd, P.S., Heijnis, H., Saunders, K.M., Simpson, G.L., Zawadzki, A., 2018. Variance and rate-of-change as early warning signals for a critical transition in an aquatic ecosystem state: a test case from Tasmania, Australia. J. Geophys. Res.: Biogeosci. 123, 495–508. https://doi.org/10.1002/2017JG004135.
Belle, S., Baudrot, V., Lami, A., Musazzi, S., Dakos, V., 2017. Rising variance and abrupt shifts of subfossil chironomids due to eutrophication in a deep subalpine lake. Aquat. Ecol. 51, 307–319.
Bestelmeyer, B.T., Ellison, A.M., Fraser, W.R., Gorman, K.B., Holbrook, S.J., Laney, C.M., Ohman, M.D., Peters, D.P.C., Pillsbury, F.C., Rassweiler, A., Schmitt, R.J., Sharma, S., 2011. Analysis of abrupt transitions in ecological systems. Ecosphere 2 (12), 1–26.
Blaauw, M., Christen, J.A., 2011. Flexible paleoclimate age-depth models using an autoregressive gamma process. Bayes. Anal. 6 (3), 457–474.
Boettiger, C., Ross, N., Hastings, A., 2013. Early warning signals: the charted and uncharted territories. Theor. Ecol. 6 (3), 255–264.
Booth, R.K., Jackson, S.T., Sousa, V.A., Sullivan, M.E., Minckley, T.A., Clifford, M.J., 2012. Multi-decadal drought and amplified moisture variability drove rapid forest community change in the humid region. Ecology 93 (2), 219–226.
Bronk Ramsey, C.B., 2009. Bayesian analysis of radiocarbon dates. Radiocarbon 51 (1), 337–360.
Bunting, L., Levitt, P.R., Simpson, G.L., Wissel, B., Laird, K.R., Cumming, B.F., St Amand, A., Engstrom, D.R., 2016. Increased variability and sudden ecosystem state change in Lake Winnipeg, Canada, caused by 20th century agriculture. Limnol. Oceanogr. 61, 2090–2107.
Carpenter, S.R., Booth, E.G., Kucharik, C.J., 2017. Extreme precipitation and phosphorus loads from two agricultural watersheds. Limnol. Oceanogr. https://doi.org/10.1002/lno.10767.
Carpenter, S.R., Brock, W.A., 2006. Rising variance: a leading indicator of ecological transitions. Ecol. Lett. 9, 311–318.

Carpenter, S.R., Cole, J.J., Pace, M.L., Batt, R., Brock, W.A., Cline, T., Coloso, J., Hodgson, J.R., Kitchell, J.F., Seekell, D.A., Smith, L., Weidel, B., 2011. Early warnings of regime shifts: a whole-ecosystem experiment. Science 332 (6033), 1079–1082.
Carstensen, J., Telford, R.J., Birks, J.B., 2013. Diatom flickering prior to regime shift. Nature 498, E11–E12.
Chen, N., Jayaprakash, C., Yu, K., Guttal, V., 2018. Rising variability, not slowing down, as a leading indicator of stachastically driven abrupt transition in a dryland ecosystem. Am. Nat. 191 (1), E1–E14.
Cimatoribus, A.A., Drijfhout, S.S., Livina, V., van der Schrier, G., 2013. Dansgaard-Oeschger events: bifurcation points in the climate system. Clim. Past 9, 323–333.
Dai, L., Vorselen, D., Korolev, K.S., Gore, J., 2012. Generic indicators of loss of resilience before a tipping point leading to population collapse. Science 336, 1175–1177.
Dakos, V., Carpenter, S.R., Brock, W.A., Ellison, A.M., Guttal, V., Ives, A.R., Kéfi, S., Livina, V., Seekell, D.A., van Nes, E.H., Scheffer, M., 2012. Methods for detecting early warnings of critical transitions in time series illustrated using simulated ecological data. PLoS One 7 (7), 1–20.
Dakos, V., Scheffer, M., van Nes, E.H., Brovkin, V., Petoukhov, V., Held, H., 2008. Slowing down as an early warning signal for abrupt climate change. Proc. Natl. Acad. Sci. U.S.A. 105, 14308–14312.
Davis, M.B., Moeller, R.E., Ford, J., 1984. Sediment focusing and pollen influx. In: Haworth, E.Y., Lund, Y.W.G. (Eds.), Lake Sediments and Environmental History. Leicester University Press, Leicester, United Kingdom, pp. 261–293.
Dietze, M.C., Fox, A., Beck-Johnson, L., Betancourt, J., Hooten, M.B., Jarnevich, C.S., Keitt, T.H., Kenney, M.A., Laney, C.M., Larsen, L.G., Loescher, H.W., Lunch, C.K., Pijanowski, B.C., Randerson, J.T., Read, E.K., Tredennick, A.T., Vargas, R., Weathers, K.C., White, E.P., 2018. Iterative near-term ecological forecasting: needs, opportunities, and challenges. Proc. Natl. Acad. Sci. Unit. States Am. 115 (7), 1424–1432. https://doi.org/10.1073/pnas.1710231115.
Ditlevsen, P.D., Johnsen, S.J., 2010. Tipping points: early warning and wishful thinking. Geophys. Res. Lett. 37, L19703.
Einarsson, A., Hauptfleisch, U., Leavitt, P.R., Ives, A.R., 2016. Identifying consumer-resource population dynamics using paleoecological data. Ecology 97 (2), 361–371.
Eldridge, D.J., Bowker, M.A., Maestre, F.T., Roger, E., Reynolds, J.F., Whitford, W.G., 2011. Impacts of shrub encroachment on an ecosystem structure and functioning: towards a global synthesis. Ecol. Lett. 14, 709–722.
Frossard, V., Saussereau, B., Perasso, A., Gillet, F., 2015. What is the robustness of early warning signals to temporal aggregation? Front. Ecol. Evolut. 3, 112. https://doi.org/10.3389/fevo.2015.00112.
Gavin, D.G., Oswald, W.W., Wahl, E.R., Williams, J.W., 2003. A statistical approach to evaluating distance metrics and analog assignments for pollen records. Quat. Res. 20, 356–367.
Goring, S., Williams, J.W., Blois, J.L., Jackson, S.T., Paciorek, C.J., Booth, R.K., Marlon, J.R., Blaauw, M., Christen, J.A., 2012. Deposition ties in the northeastern United States during the Holocene: establishing valid priors for Bayesian age models. Quat. Sci. Rev. 48, 54–60.
Hastings, A., Wysham, D.B., 2010. Regime shifts in ecological systems can occur with no warning. Ecol. Lett. 13, 464–472.
Hughes, T.P., Carpenter, S., Rockström, J., Scheffer, M., Walker, B., 2013. Multiscale regime shifts and planetary boundaries. Trends Ecol. Evol. 28 (7), 389–395.
Kéfi, S., Dakos, V., van Nes, E.H., Rietkerk, M., 2013. Early warning signals also precede non-catastrophic transitions. Oikos 122, 641–648.
Lenton, T.M., 2011. Early warning of climate tipping points. Nat. Clim. Change 1, 201–209.
Lenton, T.M., Held, H., Kriegler, E., Hall, J.W., Lucht, W., Rahmstorf, S., Schellnhuber, H.J., 2008. Tipping Elements in the Earth's climate system. Proc. Natl. Acad. Sci. Unit. States Am. 105 (6), 1786–1793.
Lenton, T.M., Livina, V.N., Dakos, V., van Nes, E.H., Scheffer, M., 2012. Early warning of climate tipping points from critical slowing down: comparing methods to improve robustness. Phil. Trans.: Math., Phys. Eng. Sci. 370 (1962), 1185–1204.
Livina, V.N., Lenton, T.M., 2007. A modified method for detecting incipient bifurcations in a dynamical system. Geophys. Res. Lett. 34, L03712. https://doi.org/10.1029/2006GL028672.
Minckley, T.A., Shriver, R.K., Shuman, B., 2012. Resilience and regime change in a southern Rocky Mountain ecosystem during the past 17000 years. Ecol. Monogr. 82 (1), 49–68.
Mudelsee, M., 2014. Climate Time Series Analysis: Classical Statistical and Bootstrap Methods, vol. 51. Springer, Dordrecht, Switzerland. https://doi.org/10.1007/978-3-319-04450-7.
Nelson, D.M., Hu, F.S., 2008. Patterns and drivers of Holocene vegetational change near the prairie-forest ecotone in Minnesota: revisiting McAndrews' transect. New Phytol. 179, 449–459.
Nelson, D.M., Hu, F.S., Tian, J., Stefanova, I., Brown, T.A., 2004. Response of C3 and C4 plants to middle-Holocene climatic variation near the prairie-forest ecotone of Minnesota. Proc. Natl. Acad. Sci. Unit. States Am. 101 (2), 562–567.
Pace, M.L., Batt, R.D., Buelo, C.D., Carpenter, S.R., Cole, J.J., Kurtzweil, J.T., Wilkinson, G.M., 2017. Reversal of a cyanobacterial bloom in response to early warnings. Proc. Natl. Acad. Sci. Unit. States Am. 114, 352–357.
Peretti, C.T., Munch, S.B., 2012. Regime shift indicators fail under noise levels commonly observed in ecological systems. Ecol. Appl. 22, 1772–1779.
Priyadarshana, W.J.R.M., Sofronov, G., 2016. Breakpoint: an R Package for Multiple Break-point Detection via the Cross-Entropy Method. R package version 1.2. https://CRAN.R-project.org/package=breakpoint.
R Core Team, 2017. R: A Language and Environment for Statistical Computing. R Foundation for Statistical Computing, Vienna, Austria. URL. https://www.R-project.org/.
Randsalu-Wendrup, L., Conley, D.J., Carstensen, J., Fritz, S.C., 2016. Paleolimnological records of regime shifts in lakes in response to climate change and anthropogenic activities. J. Paleolimnol. 56, 1–4.
Ratajczak, Z., D'Odorico, P., Nippert, J.B., Collins, S.L., Brunsell, N.A., Ravi, S., 2017. Changes in spatial variance during a grassland to shrubland state transition. J. Ecol. 105, 750–760.
Ratajczak, Z., Carpenter, S.R., Ives, A.R., Kucharik, C.J., Ramiadantsoa, T., Stegner, M.A., Williams, J., Zhang, J., Turner, M.G., 2018. Abrupt changes in ecological systems: inference and diagnosis. Trends Ecol. Evol. https://doi.org/10.1016/j.tree.2018.04.013.
Rehfeld, K., Marwan, N., Heitzig, J., Kurths, J., 2011. Comparison of correlation analysis techniques for irregularly sampled time series. Nonlinear Process Geophys. 18, 389–404.
Rindi, L., Bello, M.D., Dai, L., Gore, J., Benedetti-Cecchi, L., 2017. Direct observation of increasing recovery length before collapse of a marine benthic ecosystem. Nat. Ecol. Evolut. 1, 0153.
Sankaran, M., Hanan, N.P., Scholes, R.J., Ratnam, J., Augustine, D.J., Cade, B.S., Gignoux, J., Higgins, S.I., Le Roux, X., Ludwig, F., Ardo, J., Banyikwa, F., Bronn, A., Bucini, G., Caylor, K.K., Coughenour, M.B., Diouf, A., Ekaya, W., Feral, C.J., February, E.C., Frost, P.G.H., Hiernaux, P., Hrabar, H., Metzger, K.L., Prins, H.H.T., Ringrose, S., Sea, W., Tews, J., Worden, J., Zambatis, N., 2005. Determinants of woody cover in African savannas. Nature 438, 846–849.
Scheffer, M., Carpenter, S.R., Dakos, V., van Nes, E.H., 2015. Generic indicators of ecological resilience: inferring the chance of a critical transition. Annu. Rev. Ecol. Evol. Syst. 46, 145–167.
Scheffer, M., Bascompte, J., Brock, W.A., Brovkin, V., Carpenter, S.R., Dakos, V., Held, H., van Nes, E.H., Rietkerk, M., Sugihara, G., 2009. Early-warning signals for critical transitions. Nature 461, 53–59.
Scheffer, M., Carpenter, S., Foley, J.A., Folke, C., Walker, B., 2001. Catastrophic shifts in ecosystems. Nature 413, 591–596.
Seddon, A.W.R., Macias-Fauria, M., Willis, K.J., 2015. Climate and abrupt vegetation change in Northern Europe since the last deglaciation. Holocene 25 (1), 25–36.
Seddon, A.W.R., Froyd, C.A., Witkowski, A., Willis, K.J., 2014. A quantitative framework for analysis of regime shifts in a Galápagos coastal lagoon. Ecology 95 (11), 3046–3055.
Silverman, B.W., 1986. Density Estimation. Chapman and Hall, London, England.
Simpson, G.L., Oksanen, J., 2016. Analogue: Analogue Matching and Modern Analogue Technique Transfer Function Models. R package version 0.17-0. http://cran.r-project.org/package=analogue.
Simpson, G.L., 2007. Analogue methods in palaeoecology: using the analogue package. J. Stat. Software 22 (2), 1–29.
Smol, J.P., Wolfe, A.P., Birks, H.J.B., Douglas, M.S.V., Jones, V.J., Korhola, A., Pienitz, R., Rühland, K., Sorvari, S., Antoniades, D., Brooks, S.J., Fallu, M.-A., Hughes, M., Keatley, B.E., Laing, T.E., Michelutti, N., Nazarova, L., Nyman, M., Paterson, A.M., Perren, B., Quinlan, R., Rautio, M., Saulnier-Talbot, E., Siitonen, S., Solovieva, N., Weckström, J., 2005. Climate-driven regime shifts in the biological communities of arctic lakes. Proc. Natl. Acad. Sci. Unit. States Am. 102 (12), 4397–4402. https://doi.org/10.1073/pnas.0500245102.
Spanbauer, T.L., Allen, C.R., Angeler, D.G., Eaton, T., Fritz, S.C., Garmestani, A.S., Nash, K.L., Stone, J.R., 2014. Prolonged instability prior to regime shift. PLoS One 9 (10), e108936.
Spanbauer, T.L., Allen, C.R., Angeler, D.G., Eason, T., Fritz, A.C., Garmestani, A.S., Nash, K.L., Stone, J.R., Stow, C.A., Sundstrom, S.M., 2016. Body size distributions signal a regime shift in a lake ecosystem. Proceedings of the Royal Society B 283, 20160249.
Staal, A., Dekker, S.C., Hirota, M., van Nes, E.H., 2015. Synergistic effects of drought and deforestation on the resilience of the south-eastern rainforest. Ecol. Complex. 22, 65–75.
Staver, C.A., Levin, S.A., 2012. Integrating theoretical climate and fire effects on savannah and forest systems. Am. Nat. 180 (2), 211–224.
Steele, J.H., 1985. A comparison of terrestrial and marine ecological systems. Nature 313, 355–358.
Steffen, W., Broadgate, W., Deutsch, L., Gaffney, O., Ludwig, C., 2015a. The trajectory of the anthropocene: the Great acceleration. Anthropocene Rev. 2, 81–98.
Steffen, W., Richardson, K., Rockström, J., Cornell, S.E., Fetzer, I., Bennett, E.M., Biggs, R., Carpenter, S.R., de Vries, W., de Wit, C.A., Folke, C., Gerten, D., Heinke, J., Mace, G.M., Persson, L.M., Ramanathan, V., Reyers, B., Sörlin, S., 2015b. Planetary boundaries: guiding human development on a changing planet. Science 347, 746.
Taranu, Z.E., Carpenter, S.R., Frossard, V., Jenny, J.-P., Thomas, Z., Vermaire, J.C., Perga, M.-E., 2018. Can we detect ecosystem critical transitions and signals of changing resilience from paleo-ecological records? Ecosphere 9, e02438.
Thomas, Z., 2016. Using natural archives to detect climate and environmental tipping point in the Earth System. Quat. Sci. Rev. 152, 60–71.
Thomas, Z.A., Kwasniok, F.K., Boulton, C.A., Cox, P.M., Jones, R.T., Lenton, T.M., Turney, C.S.M., 2015. Early warnings and missed alarms for abrupt monsoon transitions. Clim. Past 11, 1621–1633.
van Nes, E.H., Staal, A., Hantson, S., Holmgren, M., Pueyo, S., Bernardi, R.E., Flores, B.M., Xu, C., Scheffer, M., 2018. Fire forbids fifty-fifty forest. PLoS One. https://doi.org/10.1371/journal.pone.0191027.
Veraart, A.J., Faassem, E.J., Dakos, V., van Nes, E.H., Laijrling, M., Scheffer, M., 2012.

Recovery rates reflect distance to a tipping point in a living system. Nature 481, 357–359.
Wang, Q., Yang, X., Anderson, N.J., Zhang, E., Li, Y., 2014. Diatom response to climate forcing of a deep, alpine lake (Lugu Hu, Yunnan, SW China) during the Last Glacial Maximum and its implications for understanding regional monsoon variability. Quat. Sci. Rev. 86, 1–12.
Webb III., T., 1993. Constructing the past from late-Quaternary pollen data: temporal resolution and a zoom lens space-time perspective. In: Kidwell, S.M., Behrensmeyer, A.K. (Eds.), Taphonomic Approaches to Time Resolution in Fossil Assemblages. Paleontological Society, Knoxville, TN, pp. 79–101.
Wilkinson, G.M., Carpenter, S.R., Cole, J.J., Pace, M.L., Batt, R.D., Buelo, C.D., Kurtzweil, J.T., 2018. Early warning signals precede cyanobacterial blooms in multiple whole-lake experiments. Ecol. Monogr. https://doi.org/10.1002/ecm.1286.
Wilks, D.S., 1995. Statistical Methods in the Atmospheric Sciences. Academic Press, London, United Kingdom.
Williams, J.W., Blois, J.L., Shuman, B.N., 2011. Extrinsic and intrinsic forcing of abrupt ecological change: case studies from the late Quaternary. J. Ecol. 99, 664–677.
Williams, J.W., Shuman, B., Bartlein, P.J., 2009. Rapid response of the prairie-forest ecotone to early Holocene aridity in mid-continental North America. Glob. Planet. Chang. 66, 195–207.
Wolkovich, E.M., Cook, B.I., McLauchlan, K.K., Davies, T.J., 2014. Temporal ecology in the anthropocene. Ecol. Lett. 17, 1365–1379.